Original Article

X-ray Micro-Computed Tomography Characterization of Autologous Teeth Particle Used in Postextraction Sites for Bone Regeneration. An Experimental Study in Dogs

José Luis Calvo-Guirado, Felix de Carlos-Villafranca[1], Miguel Garcés-Villalá[2], Nuria García-Carrillo[3], Vidushi Jindal[4], Francisco Martínez-Martinez[5]

Associate Researcher, Universidad Autónoma de Chile, Researcher of Instituto Murciano de Investigaciones Biomédicas Virgen de la Arrixaca (IMIB), Private Practice, [3]Veterinarian and Researcher of Instituto Murciano de Investigaciones Biomédicas Virgen de la Arrixaca (IMIB), [4]Private Researcher, [5]Department of Traumatology, Faculty of Medicine University of Murcia, Hospital Clínico Universitario Virgen de la Arrixaca, Instituto Murciano de Investigaciones Biomédicas Virgen de la Arrixaca (IMIB), El Palmar, Murcia, [1]Department of Orthodontics, Faculty of Medicine, University of Oviedo, Asturias, Spain, [2]Department of Implant and Biomaterial Research, Fundación Corazon de Jesús, San Juan, Argentina

Abstract

Objectives: The objective of this study was to develop a new computed method to characterize and measure the bone density measured in Hounsfield units (HU) of particulate tooth grafts, evaluated by micro-computed tomography (micro-CT) at 2 months of healing. **Materials and Methods:** Thirty-two dog teeth were crushed with a smart dentin grinder, later implanted in postextraction sites of 4 beagle dogs. Twenty-four cores were taken after 2 months and analyzed by micro-CT (Albira). The methodology used was based on a descriptive statistic of the bone density values measured in HU obtained from the creation of volumes of interest (VOIs) and predefined three-dimensional iso-contours from the images obtained after performing micro-CT of the biopsies of the crushing tooth. **Results:** The micro-CT allows established the characteristics of the biomaterials by studying the HU. The most predominant type of bone was type D3 density (400–800 HU). There was a light presence of bone-type density D2 and D1 in 2 of the regions studied. **Conclusions:** Micro-CT could be considered a technique of great value in the characterization of biomaterials based on the HU, after implantation in an *in vivo* model. The distribution of D1 and D2 particles were located around the bottom and middle part of the alveoli and the D3 and D4 bone particles were in the hole core. Therefore, the method proposed in this study is useful to determine the density of the tooth granulate (dentin grinder) and any other biomaterial.

Keywords: "Bone density," "bone graft substitute," autologous grafting, dentin graft, micro-computed tomography, particulate dentin graft, socket preservation, tooth derived bone graft

Introduction

One of the most worldwide procedures is the extraction, and teeth are still considered clinical residue and, therefore, are discarded. The healing process of bone sites results in significant changes to the ridge contour and alveolar bone loss in three dimensional (3D). This is mainly due to the relative osseous density differences.[1,2] Most of this accelerated bone loss occurs during the first 3 months following tooth extraction and gradually slows down over the ensuing months.[2] Many biomaterials have been used in dental surgery and a variety of new biomaterials have been marketed for maxillofacial, implant, and periodontal surgery. Graft biomaterials are used to repair hard and soft tissue defects. In general, extracted teeth have been discarded as infectious medical waste in the world. Most of the nonfunctional teeth are an ideal native resource to be grafted immediately.[3,4] The human demineralized dentin matrix, from extracted crushed human teeth, was developed in 2008 for its osteoconductive and remodeling capacity in implant dentistry. Bone and dentin are made up of body fluid (10%), collagen (30%), and hydroxyapatite (60%) by weight.[3] Dentin is an acellular matrix rich in collagen without vessels, whereas bone is a cellular tissue with vessels. Enamel consists of 96% inorganic substances and

Access this article online

Quick Response Code:

Website:
www.ijds.in

DOI:
10.4103/ijds.ijds_138_21

4% water, while dentin has 65% inorganic substances, 35% organic substances, and water. Cement is made up of 45%–50% inorganic substances, 50%–55% organic substances, and water. Finally, the alveolar bone has 65% inorganic substances and 35% organic substances.[3-5]

A "smart dentin grinder TM" was designed to grind and classify the extracted teeth into a specific size dentin particle. A chemical cleaner was applied to process the dentin particles in a bacterium free for 15–20 minutes.[6] Its novel procedure is indicated mainly in cases in which teeth are extracted for periodontal reasons and partially or impacted teeth. Teeth that have had root canal fillings should not be used in this procedure due to foreign material contamination.[7-11]

Medical imaging has become an essential field to address the diagnostic and therapeutic needs of our patients. Its enormous innovation in all areas of biomedicine aims to obtain crucial data and information that are integrated and used by different professionals to optimize the clinical practice of different medical disciplines.[12]

Computed tomography (CT) uses an x-ray source that rotates around the object of study to obtain images in cross-sections that allow the reconstruction of a more precise image than with classic radiographs. Since 1972, the technique has evolved and there are currently three types of CT: medical CT, dental or cone beam computerized tomography, and micro-CT.[13]

The obtaining of the image is produced thanks to logarithmic calculations that analyze the radiation through detectors, providing the radiation attenuation coefficient at each determined point, decomposing the analyzed structures into units called voxels (minimum processable volumetric unit), which are equivalent to one volume. Therefore, unlike the classic radiological imaging techniques where we obtain flat images formed by pixels, CT is the only volumetric 3D technique that allows us to measure bone density available using the UH scale, obtaining 3D images made up of these voxels. Each of these voxels gives us a numerical value, the data-raw, which can be processed mathematically thanks to the software included with the tomography, to later obtain a complete and quantifiable image.[13-15]

MATERIALS AND METHODS

The study consisted of four Beagle dogs approximately 1 year old, weighing 14–15 kg each. The Ethics Committee for Animal Research of the University of Murcia approved the study protocol that followed the guidelines established by the Directive of the Council of the European Union of February 1, 2013/53/CEE, Number A1320140404.

The clinical examination determined that the dogs were in good general health. The animals were quarantined for the application of the rabies vaccine and vital.

The animals were preanesthetized with zolazepam 10% at 0.10 ml/kg and acepromazine maleate (Calmo-Neosan®,

Pfizer, Madrid) 0.12–0.25 mg/kg and medetomidine 35 lg/kg (Medetor 1 mg, Virbac, CP-Pharma Handelsgesellschaft GmbH, Germany). The mixture was injected intramuscularly into the quadriceps femoris. The animals were taken to the operating room where, at the first opportunity, an intravenous catheter (diameter 22 or 20 G) was inserted into the cephalic vein, and propofol infusion was administered at a rate of 0.4 mg/kg/min as a constant slow infusion rate.

Anesthetic maintenance was performed with volatile anesthetics and the animals were subjected to tracheal intubation with a Magill probe for adaptation of the anesthetic device and the administration of volatile isoflurane diluted in oxygen (2V%). In addition, local anesthesia (Articaine 40 mg, 1% epinephrine, Normon®, Madrid, Spain) was administered at the surgical sites. These procedures were carried out under the supervision of a veterinary surgeon.

Mandibular premolars and first molars (P2, P3, P4, M1) were extracted bilaterally [Figure 1] under general anesthesia. Multi-rooted teeth were sectioned in a buccolingual direction at the bifurcation using a Tungsten carbide bur so that the roots could be extracted individually, without damaging the remaining bone walls.

Clean and dried teeth were immediately ground using the specially designed "Smart Dentin Grinder" for this procedure. The tooth particles that were obtained were 300–1200 um, which were subsequently sieved through a special classification system in two compartments [Figure 2].

The crushed teeth were dipped in a basic alcohol cleanser in a sterile container to dissolve all organic debris and bacteria for 15 min. The particles were partially demineralized with ethylenediaminetetraacetic acid for 2 min and are then cleaned with buffered saline for 5 min following Kometabio Company (Fort Lee, NJ, USA) indications [Figures 3 and 4].[7]

After extraction of the premolars 3 and 4 and first molar, alveoli were filled with freshly extracted crushed teeth, while the premolar 2 postextraction alveoli on both sides

Figure 1: Lower premolars P2, P3, P4, and first molar M1 of hemi mandible extracted sites for bone regeneration

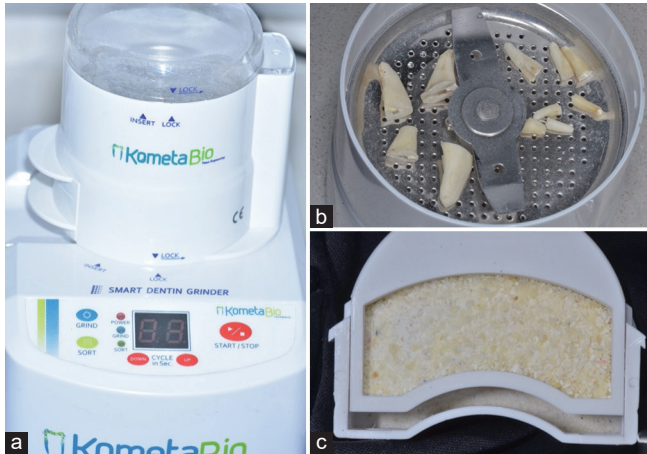**Figure 2:** Extracted teeth before grinding

Figure 3: (a) Smart Dentin Grinder machine using for the study, (b) teeth roots inside smart dentin grinder chamber, (c) tooth particles obtained after grinding

Figure 4: (a) Particulate teeth were dipped in a crystal recipient, (b) basic alcohol cleanser (red cup), Ethylenediaminetetraacetic acid (blue cap), and saline (green cap) were used for teeth cleaning and disinfection

remained untreated and allowed to heal naturally (Control Group) [Figure 5].

All surgery was performed under the supervision of the veterinarian assigned to the Animal Research Unit of the University of Murcia. Silk sutures (3-0 TB-15, Lorca Marin® Ref. 55346) were used to cover the grafted areas. Stitches were removed after 2 weeks. Throughout the surgical procedure, the intravenous line was hydrated with (glucose-saline) (250 cm³) to aid the postsurgical recovery of the animals. The following anti-inflammatory, analgesic, and antimicrobial drugs were administered: Voren® anti-inflammatory (dexamethasone isonicotinic), 1–2 ml intramuscularly and Antibiotic

Bivamox® (amoxicillin), 2 ml intramuscularly. The antibiotic and the anti-inflammatory were administered after surgery and every other day for 4 days to prevent postoperative infection and inflammation, following the guidelines established by the animal research ethics committees. The animals received antibiotics twice a day (Amoxicillin 500 mg Clamoxyl® L. A., Pfizer, Madrid).

After surgery, the dogs were transferred to each of their cages where they remained under veterinary supervision. During the days following surgery, postextraction wounds were postsurgical care to avoid infection and the general health of the animals was monitored. The animals were fed ad-libitum with a soft diet.

The oral mucosa was disinfected and cleaned with gauze soaked in a Sea 4 seawater-based mouthwash (Blue Sea Laboratories, Alicante, Spain). This procedure is always the same in Murcia Animal Research Department when you work with dogs. Periapical radiographs were taken after 2 months of healing [Figure 6].

At 2 months of healing, a local anesthetic was applied to the vestibular and lingual gums and a crestal incision was made in the regenerated area from the canine to the second molar. A full-thickness flap was lifted and using a 3 mm diameter trephine, three biopsies were taken from the control points and regenerated bone at 60 days on the left and right sides, respectively, six in total [Figure 7].

The bone cores used were scanned after the surgical intervention using an Albira trimodal preclinical scanner (Bruker®, Massachusetts, USA) obtaining an image with a resolution of less than 0.05 mm and its reconstruction in 3D [Figures 8 and 9]. The acquisition parameters are summarized in Table 1.

Measurements were calculated using a medical imaging data examiner (Amide, UCLA University, LA, USA). A global description of all statistical values was made including mean, standard deviation, median, minimum value, maximum value, size of the VOI (volume of interest) in mm³, voxel fraction, and total voxels.

An analysis of both the biomaterials and the biopsies was performed, calculating the percentages of Hounsfield units (HU) that characterized the samples by determining predefined volumes and creating individual iso-contours following the subjective classification of bone quality and volume proposed by Lekholm and Zarb in 1985 and its subsequent modification by Misch based on the location, composition, and type of density measurable by computed tomography, in which 4 types of bone are differentiated: D4 (200–400 HU), D3 (400–800 HU), D2 (800–1000 HU) and D1 (>1000 HU).

In our case, we start from 200 HU as the minimum density value in D4 to avoid selecting excess material does not equivalent to the sample. The measurement method developed is presented as follows:
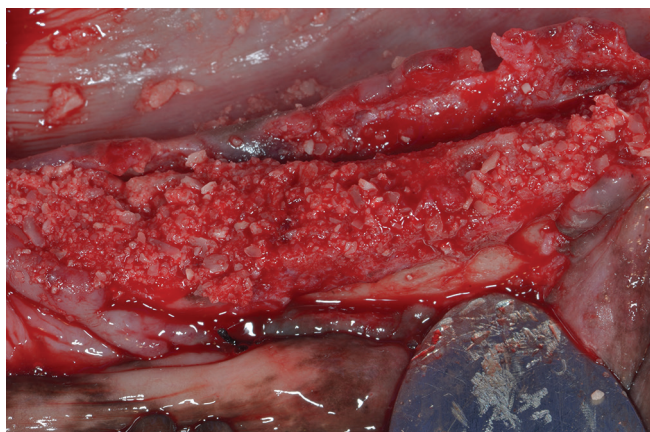
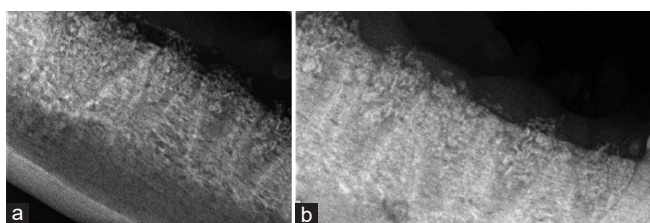**Figure 5:** Particulate teeth placed in all alveoli except premolar two

Figure 6: (a) Periapical radiographs immediately after filling, (b) Periapical radiograph after 2 months of healing showing complete bone reconstruction
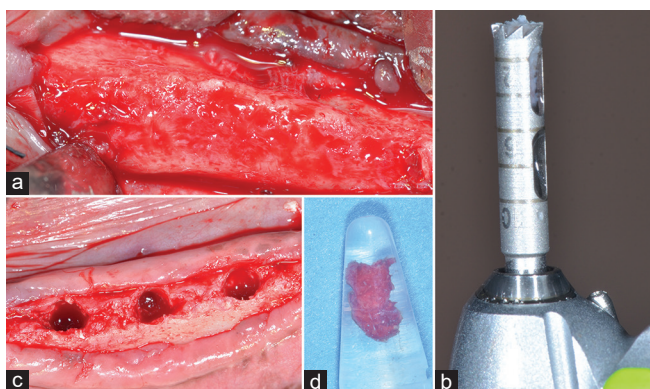

Figure 7: (a) Mandibular healed bone after 2 months with dentin graft, (b) 3 mm trephine use for core extraction, (c) three bone cores in each mandible obtained after grafting with particulate teeth, (d) bone core after dentin graft

Biomaterial analysis, evaluated following the following sequence:
1. Creation of 3D iso-contours of the samples determining a minimum HU value for the creation of VOIs (volume of interest) following the classification [Table 2].

These volume delimited VOIs are statistically analyzed by the above-mentioned examiner (AMIDE Medical Imaging Data Examiner). Next, the biopsies were studied applying the same measurement protocols as for the individual samples, with slight modifications due to the size and heterogeneity of the samples [Figure 10].

Table 1: Micro-computed tomography acquisition parameters (own design for each biomaterial)

Data	Values
Voltage (kV)	46
Intensity (mA)	0.3
Dosis (mA)	0.4
Voxels size (mm)	0.05
High resolution (projections)	600
Digital flat panel (pixels)	2401×2401
Field of view (mm)	80×80
Reconstructed	FBP

FBP: Filtered backprojection algorithm

Table 2: Different isocontour of bone density

Isocontour 3D VOI 0.2 (200 HU)
Isocontour 3D VOI 0.35 (400 HU)
Isocontour 3D VOI 0.85 (800 HU)
Isocontour 3D VOI 1.25 (1000 HU)

VOI: Volumes of interest, HU: Hounsfield units

Statistical analysis

Values were recorded as mean-standard deviation. If the distribution of two paired variables in two related samples is the same, the test considers the magnitude of the differences between those two paired variables. Equal means were considered as null hypotheses, while the existence of significant differences between means acted as an alternative hypothesis. As significant differences between the existing means, the null hypothesis was rejected. All data were expressed as mean means and standard deviation. Statistical analysis was performed using SPSS 15.0 software (SPSS, Chicago, IL, USA). Significance was established as $P < 0.05$.

RESULTS

Dentin grinder

After 2 months of healing, twenty-four postregeneration cores of dentin graft we obtained that the most newly bone formed was Density D3, followed by D2 bone, compared with another type of densities Table 3.

Return on investment (ROI) boxes were made in the middle of each dentin graft core and determined the amount of newly formed bone on top, middle, and at the bottom of each core to determine the quality of bone in different areas [Figure 11].

We can observe how we obtain with the three boxes located at different points in the core, similar characteristics in terms of percentage of volume concerning the volume defined according to the HU [Figures 11 and 12].

The descriptive analysis showed that in the upper area of the core, most of them is related to D4 bone density (0.509% ± 0.14%); the middle area, we found D3 bone density (0.734% ± 0.22%) and the bottom D2 bone density (0.858% ± 0.33%) [Table 4].
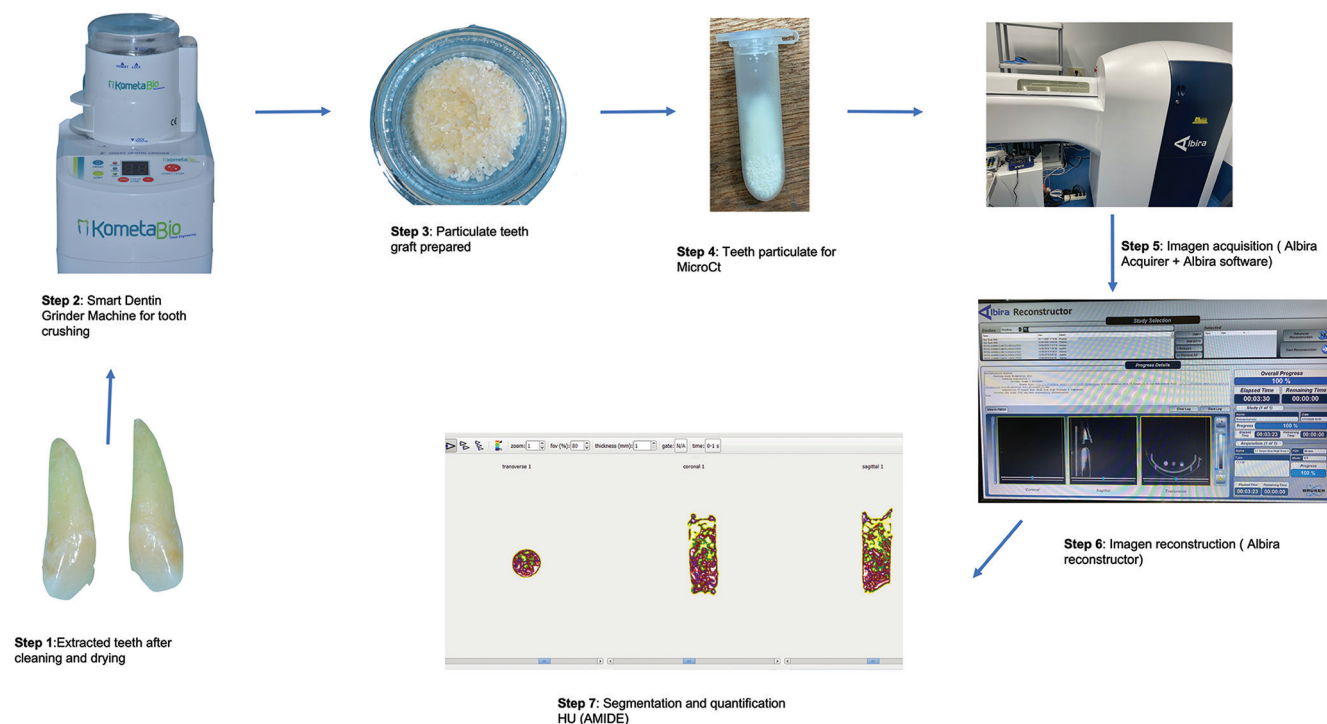
Figure 8: Diagram of different steps following for the acquisition and processing of the micro-computed tomography image in crushed teeth, (a) extracted teeth after cleaning, (b) Smart dentin grinder machine for tooth grinding, (c) particulate teeth of 1200 microns, (d) plastic tube for micro-computed tomography scan, (e) imagen acquisition (Albira Acquirer + Albira software), (f) imagen reconstruction (Albira reconstructor), (g) Segmentation and quantification (Amide Software, LA, UCLA, USA)
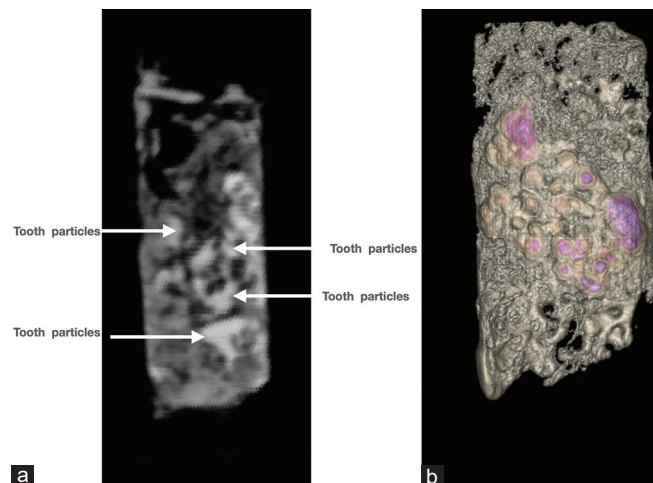

Figure 9: (a) Dentin graft core of 10 mm length after software reconstruction in which observes tooth particles inside, (b) purple dots of tooth particles included inside bone core after 2 months of healing (Volview, Kitware, Inc., New York, USA)

During the evaluation of the ROI isocontour, the AMIDE program expresses different colors of different bone densities [Table 5]. There is a marked predominance of D3 bone density (400–800) in the sample with a mean percentage of 53.89%. All data are expressed in Table 5.

The presence of bone-like density D3 predominates, coinciding with the analysis of the VOI comprised in the cylinder evaluated previously. In this last sample, we observed how the presence of D4 bone-type density predominates, unlike the volumetric analysis where a majority percentage of D2 bone-type density is present. This is due, as in the previous cases, to the presence of nonbone tissue with a density equal to or greater than 200 HU that does not belong to the sample to be evaluated. The evaluation program detects de isocontour expressed in Figure 12.

The biopsies taken after dentin graft grafts at 2 months, we can say that the previously treated tooth particles behave in different ways and are in different areas of the socket. Once the tooth particles are treated with the company disinfection method the crushed tooth particles behave differently.[16,17] Those that are not completely resorbable that form the bone of density 1 (5.39% ± 0.11%) always approach around the alveolus, toward the walls of the old bone. This tells us that they can try to reinforce the alveolus from the inside, acting as internal reinforcement of its walls.

The particles that have been reabsorbed to a lesser extent that formed the bone of density 2 (26.29% ± 0.14%) are in the biopsy in the lower middle part of the alveolus, maintaining the stability of the bone. However, the bone that has been partially resorbed the most, such as bone density 3 (53.89% ± 0.18%), which occupies most of the biopsy, is distributed throughout the interior of the biopsy and the new-formed alveolus. The one that also reabsorbs to a lesser extent is bone D4 (14.43% ± 0.03%) that we will find in the upper part of

Table 3: Descriptive statistics of Hounsfield units values belonging to the predefined volume of each box (source: Own elaboration)

Cores numbers	# ROI	Median	Mean	SD	Minimum	Maximum	Size (mm³)	Voxels
24	>200-D4	532.34	546.88	94.46	280	902.44	4.87E+02	5432
24	>400-D3	565.88	575.77	88.91	390	902.44	4.87E+02	5643
24	>800-D2	886.42	899.65	12.87	870	902.44	3.99E+00	8
24	>1000-D1	0.21	0.34	0.44	0.35	0.79	1.01E+01	4

SD: Standard deviation

Table 4: Descriptive statistics of Hounsfield units values belonging to predefined volume of each box (source: Own elaboration)

	Mean (%)	Median	SD	Minimum	Maximum	Size (mm³)	Fraction voxels	Voxels
Upper box	0.356±0.14	0.314±0.12	0.116±0.17	0.0895±0.12	146.649±0.19	1406	1406.00	2774
Middle box	0.734±0.22	0.710±0.14	0.172±0.26	0.190±0.34	139.939±0.32	1224	1224.00	2412
Bottom box	0.858±0.33	0.826±0.22	0.225±0.19	0.357±0.18	148.147±0.12	1262.25	1262.25	2484

SD: Standard deviation
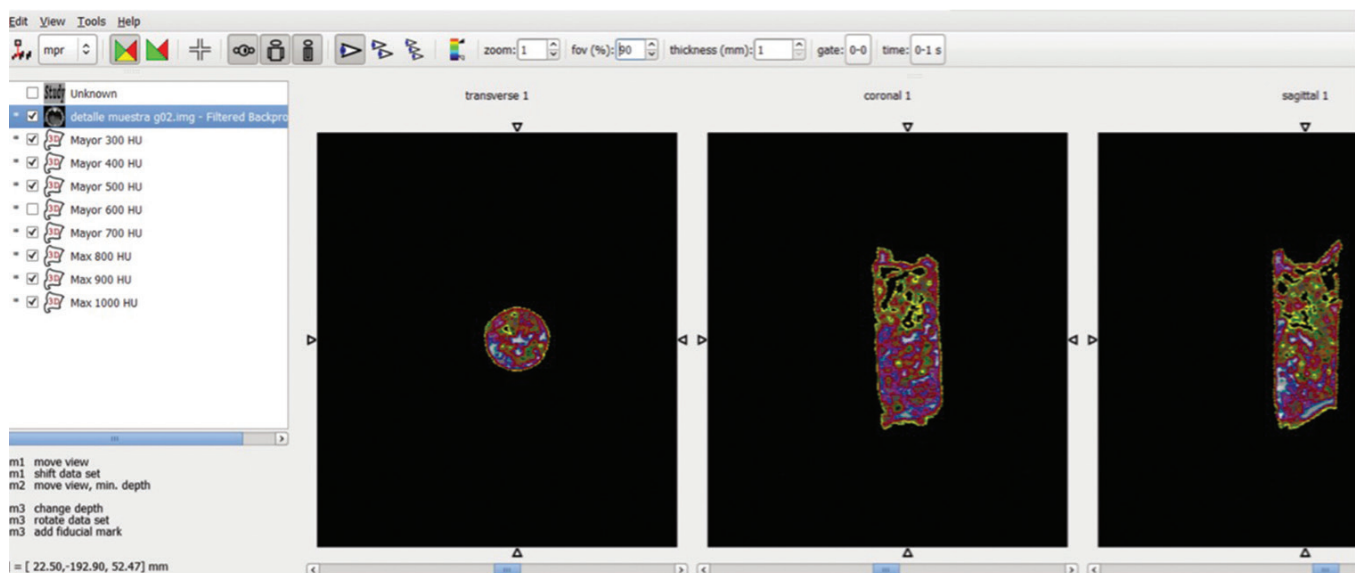
Figure 10: (a) dentin grinder transversal core image showing different types of bone densities, (b) coronal core image evaluating the most significant type of bone, (c) sagittal core image evaluating the quality of bone formed. Yellow color is related to D4 bone, Orange to D3 bone, Green to D2 bone, and Red to D1 density expressed in Hounsfield Units (Amide Software, UCLA University, LA, USA)

the biopsy where there is a greater blood supply, and more remodeling exists [Figure 13].

The main problem found in this UH quantification methodology is the impossibility of determining the minimum density present in each sample, including in some cases nontissue material to be evaluated and biasing our analysis. To avoid this, a good alternative would be to establish a predefined VOI of a size considerably smaller than the sample itself, determine its minimum UH value and use this to mark the minimum value to be measured in the creation of different boxes.

Discussion

Our results revealed that D1 bone particles of dentin graft move around the alveolus such as D2 density bone and the predominant type of bone was D3 and D4 bone in the hole core of the dentin graft. The bone graft material derived from the tooth with no antigenicity enhances the remodeling capabilities of the bone. Demineralized dentin exposes matrix-derived growth and differentiation factors for effective osteogenesis, newly formed bone, and residual demineralized dentin are weak to support implant anchorage. In contrast, our sustainable development goals procedure allows the preparation of bacteria-free particulate dentin from freshly extracted autologous teeth, ready to be used immediately as an autogenous biomaterial in the same session maintained for years.[18-26]

Until the invention of micro-CT, histology was the only effective method to evaluate the parameters of bone

microarchitecture, however, it was difficult to interpret a 3D bone structure using only two-dimensional slices.

A great advantage of micro-CT is that the sample does not need special preparation, the only requirement being the adequate size of the sample to be able to be introduced into the appropriate radiodiagnosis equipment.

In recent decades, many authors have proposed the use of micro-Ct for bone and biomaterial analysis, enhancing its value for research by increasing its availability in recent years. In general, micro-CT allows us to obtain images of bone and calcified structures with a much higher resolution than clinical CT. We can evaluate any anatomical or pathological tissue, especially bone, but we can also observe cartilage, dental tissue, and tissues filled with contrast agents to some extent.[27]
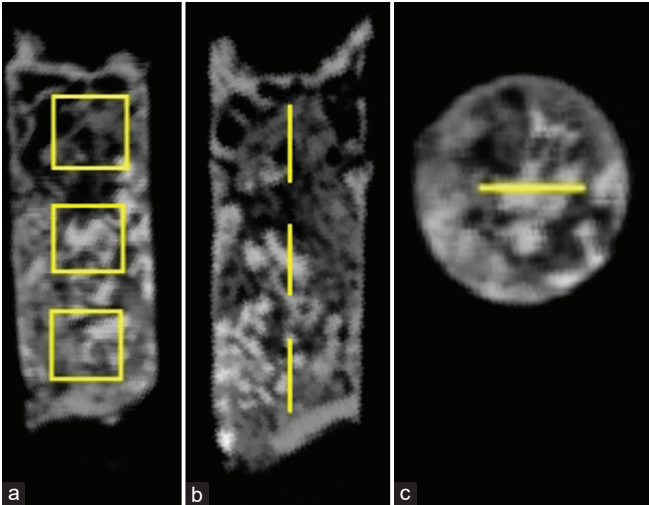

Figure 11: (a) Sagittal view of dentin core showing evaluation boxes inside, (b) transversal view of denting graft core with evaluation box inside, (c) coronal area with a control evaluation of bone density (Amide Software, UCLA University, LA, USA)

Table 5: Type of bone mean founded according to the Hounsfield units ranges in dentin cores and the estimated percentage in the biopsy (source: Own elaboration)

Micro-CT dentistry color	Density of bone (HU)	Total volume (%), mean±SD
Yellow	D4 (200-400 UH)	14.43±0.03
Orange	D3 (400-800 UH)	53.89±0.18
Green	D2 (800-1000 UH)	26.29±0.14
Red	D1 (>100 UH)	5.39±0.11

SD: Standard deviation. CT: Computed tomography, HU: Hounsfield units

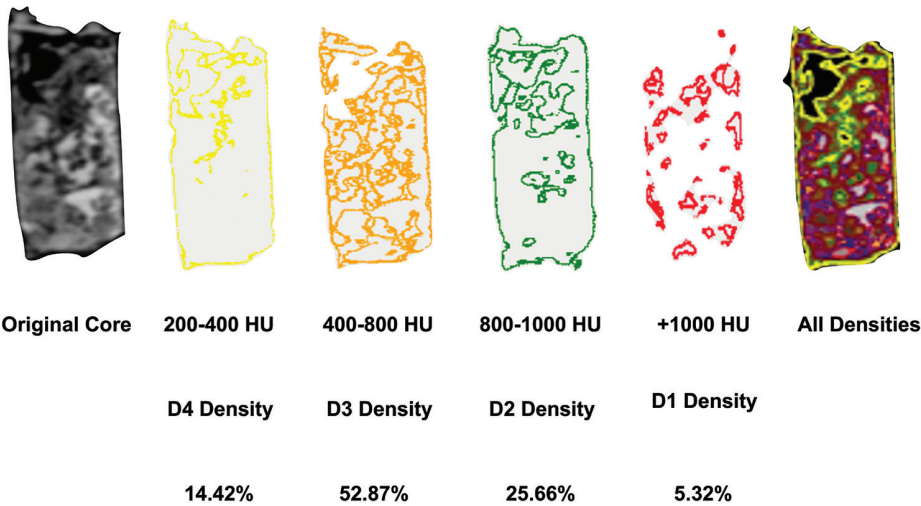| Original Core	200-400 HU	400-800 HU	800-1000 HU	+1000 HU	All Densities
	D4 Density	D3 Density	D2 Density	D1 Density	
	14.42%	52.87%	25.66%	5.32%	

Figure 12: Different isocontours depending on bone quality; yellow D4, orange D3, green D2; red D1, and all density at the end (Amide Software, UCLA University, LA, USA)
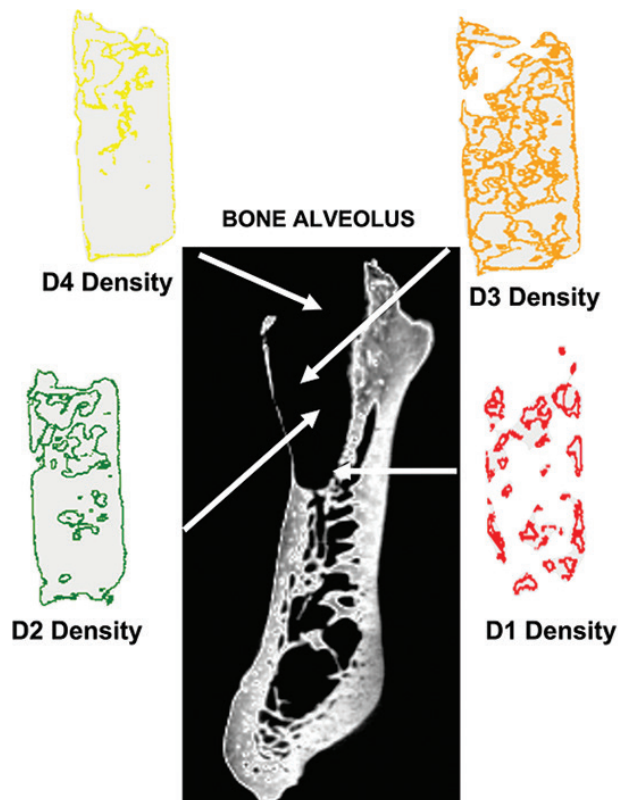
Figure 13: Type of density founded in grounded teeth grafts, related to bone location inside the alveoli

It is a technique that provides a 3D image without the need to destroy the sample, so it can be prepared and used for subsequent histological analysis, generating a complimentary analysis of the same area of tissue examined.[28,29]

Micro-CT is a technique that has been widely used in the field of medicine and dentistry to analyze the quality of bone tissue defined by various structural parameters such as its mineral properties, thus being able to evaluate bone microarchitecture through a representative bone volume.[28,29]

However, within the limitations we can highlight the small size of the sample, the high cost of the equipment, and the specificity of software programs and reconstruction algorithms, requiring some training for their management.[16] In addition, the results of the bone structure to be evaluated will be highly dependent on the size of the voxel analyzed, so it is always recommended to use equipment that presents the highest possible resolution, especially when we are going to analyze microstructure samples to obtain high precision of the results.

It must be considered that the mechanical and biological behavior of bone tissue plays a fundamental role in clinical practice, either for the evaluation of systemic or local conditions that affect the bone structure or to achieve greater compression around the bone. Bone regeneration and remodeling process as occurs for example after techniques of preservation or augmentation of the alveolar ridge.[30]

At present, micro-CT equipment is available for the evaluation of structures, and obtaining images both *in vivo* and *in vitro*, allows obtaining *in vivo* images of small animals. Alive.[31] Furthermore, using the histological study, only a few sections or sections of each implant could be obtained, being the micro-CT an ideal alternative since it shows a spatial representation of the bone formation on the surface and around the implant.

Particelli *et al*. carried out a comparison of the porosity of cortical bone samples evaluated by micro-CT and classical histology, confirming that computerized microtomography can be an effective tool to characterize the microstructure of the cortical bone.[28] Basillais *et al*. evaluated the microarchitecture of the cortical bone of the human femur through 3D analysis in micro-CT, validating the technique by comparing the structural measurements with ultrasonic techniques and scanning electron microscopy since they observed a strong correlation between the porosity obtained by the different techniques (two-dimensional and 3D).[32]

Britz *et al*. tried to validate micro-CT against histological techniques evaluating the porosity of cortical bone in rats, concluding that it is possible to measure bone porosity using high-resolution 3D equipment, not finding statistically significant differences. concerning histological analysis.[33]

Boca *et al*. concluded that micro-CT represents an interesting alternative technique to histological sectioning in the detection of caries, as it is a nondestructive, precise, and reproducible technique.[34]

Therefore, we can affirm that micro-CT provides detailed information on the trabecular bone structure and is considered the gold standard method for its evaluation and can be used to evaluate the microarchitecture of the trabecular bone and the morphology of the cortical bone. Therefore, in addition to using CBCT to analyze the shape and contours of tissues, several recent studies on the use of values on the grayscale to determine bone density using CBCT have shown a specific relationship between bone quantity and quality with these values.[35-37]

Nomura *et al*. and Hsu *et al*. demonstrated the existence of high correlations of the bone density grayscale values determined by dental CT with the bone microarchitecture parameters determined by micro-CT, concluding that dental CT can be used clinically to determine the content bone mineral and indirectly estimate the microarchitecture of trabecular bone by calculating the grayscale values of bone density.[36,37]

However, certain authors such as Pauwels *et al*. and Van Dessel *et al*. demonstrated that the ever-improving image quality of CBCT allows it to display trabecular bone patterns, indicating that it may be possible to apply structural analysis methods that are commonly used in micro-CT and histology.[13,38] Furthermore, micro-CT imaging is capable of offering detailed 3D information of periodontal structures, progression of periodontal destruction, and also the repair or regeneration process of all tissues and also dental implants.[39,40]

CBCT and micro-CT provide comparable results in the assessment of the relative difference in gray level distribution between alveolar and basal cortical bone regions in the human mandible and it can be a reliable method when assessing the degree of bone mineralization using CBCT images.[41]

In our study, we focused our analysis on the objective evaluation of densities based on the Hounsfield scale as one of the parameters necessary to determine bone quality after dentin graft implantation. This study is the creation of a method for measuring and analyzing bone cores based on the densities in HU present in preestablished VOIs (volumes of interest). We can determine bone quality by defining a series of morphometric parameters and the distribution of dentin particles related to size and orientation.

Conclusions

The quality of bone obtained by measuring the micro-CT to the crushed tooth biomaterial is like the bone of density D3 of a human being, highly qualified to be used as a biomaterial in bone defects. Micro-CT analysis has demonstrated its usefulness in a wide variety of applications in the field of dental research, being the standard gold technique to evaluate the morphometric characteristics of bone tissue as a complementary alternative to conventional histological analysis. The distribution of D1 and D2 particles was located around the bottom and middle part of the alveoli and the D3 and D4 bone particles were located in hole biopsies. Therefore, the method proposed in this study is useful to determine the density of the tooth granulate (dentin grinder), but it must be complemented with the analysis of other parameters of bone microarchitecture to be able to carry out a precise and reliable evaluation of the quality of the tooth. Bone tissue to be examined because by itself it does not fully represent it.

Ethical clearance

Ethical Comitee University of Murcia . Identification Code A1320140404.

Financial support and sponsorship

Nil.

Conflicts of interest

There are no conflicts of interest.

References

1. Schropp L, Wenzel A, Kostopoulos L, Karring T. Bone healing and soft tissue contour changes following single-tooth extraction: A clinical and radiographic 12-month prospective study. Int J Periodontics Restorative Dent 2003;23:313-23.
2. Horowitz R, Holtzclaw D, Rosen PS. A review on alveolar ridge preservation following tooth extraction. J Evid Based Dent Pract 2012;12:149-60.
3. Binderman I, Hallel G, Casp N, Yaffe A. A novel procedure to process extracted teeth for immediate grafting of autogenous dentin. J Interdiscip Med Dent Sci 2014;2:1-5. [Doi: 10.4172/2376-032X.1000154].
4. Malmgren B. Ridge preservation/decoronation. J Endod 2013;39:S67-72.
5. Valdec S, Pasic P, Soltermann A, Thoma D, Stadlinger B, Rücker M. Alveolar ridge preservation with autologous particulated dentin – A case series. Int J Implant Dent 2017;3:12.
6. Calvo-Guirado JL, Ballester-Montilla A, N De Aza P, Fernández-Domínguez M, Alexandre Gehrke S, Cegarra-Del Pino P, *et al.* Particulated, extracted human teeth characterization by SEM ‑ EDX evaluation as a biomaterial for socket preservation: An *in vitro* study. Materials (Basel) 2019;12:380.
7. Calvo-Guirado JL, Maté-Sánchez de Val JE, Ramos-Oltra ML, Pérez-Albacete Martínez C, Ramírez-Fernández MP, Maiquez-Gosálvez M, *et al.* The use of tooth particles as a biomaterial in post-extraction sockets. Experimental study in dogs. Dent J (Basel) 2018;6:12.
8. Calvo-Guirado JL, Cegarra Del Pino P, Sapoznikov L, Delgado Ruiz RA, Fernández-Domínguez M, Gehrke SA. A new procedure for processing extracted teeth for immediate grafting in post-extraction sockets. An experimental study in American Fox Hound dogs. Ann Anat 2018;217:14-23.
9. Pohl S, Binderman I, Tomac J. Maintenance of alveolar ridge dimensions utilizing an extracted tooth dentin particulate autograft and PlateletRich fibrin: A retrospective radiographic ConeBeam computed tomography study. Materials (Basel) 2020;13:1083.
10. Mele RE, Kurtzman GM, Binderman I, Mahesh L. Veterinary osseous site reconstruction utilizing autologous dentin from extracted teeth. Int J Oral Implantol Clin Res 2017;8:1-9.
11. Pohl S, Binderman I, Božić D, Shapira L, Venkataraman NT. Effectiveness of autologous tissue grafts on soft tissue ingrowth in patients following partial root extraction with socket shield: A retrospective analysis of a case series. Int J Oral Maxillofac Implants 2021;36:362-70.
12. Deserno Né Lehmann TM, Handels H, Maier-Hein Né Fritzsche KH, Mersmann S, Palm C, Tolxdorff T, *et al.* Viewpoints on medical image processing: From science to application. Curr Med Imaging Rev 2013;9:79-88.
13. Pauwels R, Jacobs R, Singer SR, Mupparapu M. CBCT-based bone quality assessment: Are Hounsfield units applicable? Dentomaxillofac Radiol 2015;44:20140238.
14. van 't Hof RJ. Analysis of bone architecture in rodents using microcomputed tomography. Methods Mol Biol 2012;816:461-76.
15. Bouxsein ML, Boyd SK, Christiansen BA, Guldberg RE, Jepsen KJ, Müller R. Guidelines for assessment of bone microstructure in rodents using micro-computed tomography. J Bone Miner Res 2010;25:1468-86.
16. Calvo-Guirado JL, Garcés-Villalá MA, Mahesh L, De Carlos-Villafranca FA. Effectiveness of chemical disinfection in discarding pathogenic bacteria of human particulate tooth graft: An *in vitro* study. Indian J Dent Sci 2021;13:277-82.
17. Calvo-Guirado JL. Temporary implants and particulate dentin graft protecting traditional implants in severe periodontal patient: A case report. Indian J Dent Sci 2021;13:201-4.
18. Park CH, Abramson ZR, Taba M Jr., Jin Q, Chang J, Kreider JM, *et al.* Three-dimensional micro-computed tomographic imaging of alveolar bone in experimental bone loss or repair. J Periodontol 2007;78:273-81.
19. Kim YK, Lee J, Um IW, Kim KW, Murata M, Akazawa T, *et al.* Tooth-derived bone graft material. J Korean Assoc Oral Maxillofac Surg 2013;39:103-11.
20. Yeomans JD, Urist MR. Bone induction by decalcified dentine implanted into oral, osseous and muscle tissues. Arch Oral Biol 1967;12:999-1008.
21. Huggins C, Wiseman S, Reddi AH. Transformation of fibroblasts by allogeneic and xenogeneic transplants of demineralized tooth and bone. J Exp Med 1970;132:1250-8.
22. Kim YK, Kim SG, Yun PY, Yeo IS, Jin SC, Oh JS, *et al.* Autogenous teeth used for bone grafting: A comparison with traditional grafting materials. Oral Surg Oral Med Oral Pathol Oral Radiol 2014;117:e39-45.
23. Sánchez-Labrador L, Martín-Ares M, Ortega-Aranegui R, López-Quiles J, Martínez-González JM. Autogenous dentin graft in bone defects after lower third molar extraction: A split-mouth clinical trial. Materials (Basel) 2020;13:3090.
24. Santos A, Botelho J, Machado V, Borrecho G, Proença L, Mendes JJ, *et al.* Autogenous mineralized dentin versus xenograft granules in ridge preservation for delayed implantation in post-extraction sites: A Randomized controlled clinical trial with an 18 months follow-up. Clin Oral Implants Res 2021;32:905-15.
25. Del Canto-Díaz A, de Elío-Oliveros J, Del Canto-Díaz M,

Alobera-Gracia MA, Del Canto-Pingarrón M, Martínez-González JM. Use of autologous tooth-derived graft material in the post-extraction dental socket. Pilot study. Med Oral Patol Oral Cir Bucal 2019;24:e53-60.

26. Al-Asfour A, Farzad P, Al-Musawi A, Dahlin C, Andersson L. Demineralized xenogenic dentin and autogenous bone as onlay grafts to rabbit tibia. Implant Dent 2017;26:232-7.

27. Rühli FJ, Kuhn G, Evison R, Müller R, Schultz M. Diagnostic value of micro-CT in comparison with histology in the qualitative assessment of historical human skull bone pathologies. Am J Phys Anthropol 2007;133:1099-111.

28. Particelli F, Mecozzi L, Beraudi A, Montesi M, Baruffaldi F, Viceconti M. A comparison between micro-CT and histology for the evaluation of cortical bone: Effect of polymethylmethacrylate embedding on structural parameters. J Microsc 2012;245:302-10.

29. Irie MS, Rabelo GD, Spin-Neto R, Dechichi P, Borges JS, Soares PB. Use of micro-computed tomography for bone evaluation in dentistry. Braz Dent J 2018;29:227-38.

30. Müller R. Bone microarchitecture assessment: Current and future trends. Osteoporos Int 2003;14 Suppl 5:S89-95.

31. Swain MV, Xue J. State of the art of Micro-CT applications in dental research. Int J Oral Sci 2009;1:177-88.

32. Basillais A, Bensamoun S, Chappard C, Brunet-Imbault B, Lemineur G, Ilharreborde B, *et al.* Three-dimensional characterization of cortical bone microstructure by microcomputed tomography: Validation with ultrasonic and microscopic measurements. J Orthop Sci 2007;12:141-8.

33. Britz HM, Jokihaara J, Leppänen OV, Järvinen T, Cooper DM. 3D visualization and quantification of rat cortical bone porosity using a desktop micro-CT system: A case study in the tibia. J Microsc 2010;240:32-7.

34. Boca C, Truyen B, Henin L, Schulte AG, Stachniss V, De Clerck N, *et al.* Comparison of micro-CT imaging and histology for approximal caries detection. Sci Rep 2017;7:6680.

35. Parsa A, Ibrahim N, Hassan B, van der Stelt P, Wismeijer D. Bone quality evaluation at dental implant site using multislice CT, micro-CT, and cone beam CT. Clin Oral Implants Res 2015;26:e1-7.

36. Hsu JT, Chen YJ, Ho JT, Huang HL, Wang SP, Cheng FC, *et al.* A comparison of micro-CT and dental CT in assessing cortical bone morphology and trabecular bone microarchitecture. PLoS One 2014;9:e107545.

37. Nomura Y, Watanabe H, Shirotsu K, Honda E, Sumi Y, Kurabayshi T. Stability of voxel values from cone-beam computed tomography for dental use in evaluating bone mineral content. Clin Oral Implants Res 2013;24:543-8.

38. Van Dessel J, Huang Y, Depypere M, Rubira-Bullen I, Maes F, Jacobs R. A comparative evaluation of cone beam CT and micro-CT on trabecular bone structures in the human mandible. Dentomaxillofac Radiol 2013;42:20130145.

39. Chang PC, Liang K, Lim JC, Chung MC, Chien LY. A comparison of the thresholding strategies of micro-CT for periodontal bone loss: A pilot study. Dentomaxillofac Radiol 2013;42:66925194.

40. González-García R, Monje F. The reliability of cone-beam computed tomography to assess bone density at dental implant recipient sites: A histomorphometric analysis by micro-CT. Clin Oral Implants Res 2013;24:871-9.

41. Taylor TT, Gans SI, Jones EM, Firestone AR, Johnston WM, Kim DG. Comparison of micro-CT and cone beam CT-based assessments for relative difference of grey level distribution in a human mandible. Dentomaxillofac Radiol 2013;42:25117764.